Chemical Physics 100 (1985) 339–354
North-Holland, Amsterdam

ROTATION OF MOLECULES AROUND SPECIFIC AXES: AXES REORIENTATION UNDER ROTATIONAL EXCITATION

I.M. PAVLICHENKOV

I.V. Kurchatov Institute of Atomic Energy, Moscow, 123182, USSR

and

B.I. ZHILINSKII [1]

Chemistry Department, Moscow State University, Moscow, 119899, USSR

Received 4 April 1985

Rotational energy levels of nearly spherical molecules in an isolated vibrational state are studied. It is shown that, in the limit of high rotational quantum number J, the rotational states may be interpreted as those of a stable rotation around axes properly oriented in the molecular frame. The orientation of the axes depends on J. Simple analytical solutions are given for the problem considered in the asymptotic and harmonic approximations. The results obtained possess a clear qualitative interpretation of the phenomena considered and, at the same time, agree quantitatively with the results of numerical diagonalization. The analogy between the effects of rearrangement of the rotational levels under the variation of J and the critical phenomena in macroscopic systems is discussed. The intensities of rovibrational transitions between totally symmetric vibrational states are calculated. A new selection rule is introduced which is due to a small overlap of the rotational functions corresponding to the rotation around differently oriented axes.

1. Introduction

Considerable progress recently made in experimental spectroscopic methods gives birth to very detailed information concerning rovibrational energy levels and electromagnetic transitions between them. The experimental rovibrational data are usually treated in terms of an effective hamiltonian including many adjustable parameters. The alternative approach is to give a reasonable qualitative interpretation by using simple models with a small number of parameters. The cluster theory of the rotational structure of molecular spectra is a good example of such an approach [1–5]. A qualitative explanation of the rotational level clustering was given by Dorney and Watson [1]. They treated states forming each cluster in the classical limit as those of a stable rotation around equivalent axes. In this approach different types of clusters correspond to different sets of equivalent stable axes of rotation. The formulation of the corresponding quantum problem and its solution for some important particular cases was given by Harter and Patterson [2–4]. In ref. [4] the useful concept of the rotational energy surfaces for asymmetric and spherical top molecules is introduced and graphically illustrated. One of the authors of the present paper developed a general approach to the description of the rotational cluster structure for the quantum problem using the irreducible tensor operator technique [5]. This approach permits us to find and give a quantitative description for clusters including states with a nearly maximal projection $|M|$ of the angular momentum on the stable axes of molecular rotation.

Rotation–vibration interactions result in the variation of the effective inertia tensor for a par-

[1] To whom correspondence should be addressed.

0301-0104/85/$03.30

ticular rotational multiplet (a group of levels with the same J) under vibrational and rotational excitations. The modifications of the inertia tensor may include: (i) the variation of the orientation of the stationary axes with respect to the molecular frame; (ii) appearance of some new axes or disappearance of some of the existing ones; (iii) the interchange of the stability of some stationary axes.

In the present work we study the influence of the abovementioned effects on the rotational energy levels and rovibrational spectra of nearly spherical tops [*].

The shift of the stationary molecular rotation axes with increasing J value generally causes regular modifications in the cluster structure of the rotational multiplet. At a fixed critical value J_0 of the rotational quantum number (and the corresponding orientation of the stationary axis) an abrupt rearrangement may occur in that part of the rotational multiplet which corresponds to the precession of the angular momentum vector J around this particular axis. We name such a phenomenon a transition by analogy to phase transitions in macroscopic systems [**]. If the orientation of the stable axis of rotation changes abruptly in passing through the critical point J_0, the first derivative of the rotational energy dE/dJ (i.e. the rotation frequency) has a discontinuity at J_0. Such a transition in the rotational band of asymmetric nuclei was studied by one of the authors in ref. [8]. This paper deals with transitions with a smooth variation of the axis orientation. It will be shown in section 3.3 that the first derivative dE/dJ is continuous at J_0 for such transitions but the second one, d^2E/dJ^2, has a jump discontinuity at J_0. The molecular symmetry is very important for these transitions. The notion of the local symmetry group for a given molecular axis being introduced, the transitions considered correspond to a broken local symmetry of the rotation axis (for example, C_2 or C_s). Therefore, the number of stable rotation axes at J_0 increases, for example, twice (see section 3.3).

The shift of the stable rotation axes results in a considerable variation of the intensities of the rovibrational transitions at high J. A new approximate selection rule arises (for $J \gg 1$) which is due to a small overlap of the rotational wavefunctions corresponding to the states with a definite nearly maximal projection of the angular momentum on differently oriented axes of stable rotation (see section 3.4).

The methods used earlier for the description of the cluster structure [2–5] were based on rather a simple diagonal approximation for the rotational hamiltonian after the appropriate choice of the quantization axis for the angular momentum. The boson expansion method [9] is more suitable for studying the critical phenomena in an isolated molecule under rotational excitation. This method is based on the Holstein–Primakoff representation [10] for the angular momentum operators. This representation is widely used in the theory of the collective motion of atomic nuclei. The harmonic boson approximation is applicable to the description of small oscillations near the equilibrium for a given dynamic system. For the problem considered the harmonic approximation is valid for the precession of the angular momentum J around the stable rotation axis. Therefore, the boson approximation enables one to find the stable axes and the critical transition point J_0. Moreover, the harmonic approximation yields rather an accurate description of the rovibrational transition probabilities by straightforward analytical calculations.

2. Rotational hamiltonian for slightly aspherical molecules and methods for its treatment

To realize the general ideas mentioned in section 1 we consider the rotational structure of a non-degenerate vibrational state of a tetrahedral

[*] Similar problems have been investigated earlier from a somewhat different point of view. Axes shifting under variation of the effective hamiltonian parameters reflecting the vibrational excitation was studied in ref. [6]. In ref. [7] the rotational structure of the electronic transition was studied in the case of electronic states with different orientation of the principal axes of the inertia tensor.

[**] Bifurcation is an analog of these phenomena in classical mechanics. The whole family of classical trajectories of the system in the phase space is qualitatively modifed in passing through the bifurcation point (see section 3.3).

molecule XY_4, assuming that its tetrahedral symmetry is slightly broken by an isotopic substitution of one or two Y atoms. Two isotopic modifications, $XY_2^*Y_2$ and XY^*Y_3, of this molecule are discussed below.

We assume that the following simple hamiltonian is sufficient for the description of the rotational structure of the isolated vibrational state:

$$H = H_{sp} + H_{asp} + tR^{4(4,A_1)}. \tag{2.1}$$

The first term H_{sp} corresponds to the rotational energy $BJ(J+1)$ of the rigid spherical top. The second one, H_{asp}, corresponds to deviations from the rigid spherical top due to the isotopic substitution. The third term takes into account the centrifugal distortion effects in the spherical molecule. This term is proportional to the tensor operator $R^{4(4,A_1)}$ of the fourth rank with respect to the SO(3) group, which is invariant with respect to the molecular cubic symmetry group. The contributions from the fourth-rank tensor operators of lower symmetry are small due to the small asphericity of the molecule.

The standard orientation of the molecular frame is suitable for the $XY_2^*Y_2$ isotopic modification (the x, y, z axes coincide with the axes S_4 of the undistorted tetrahedral XY_4 molecule). The rotational hamiltonian for the rigid asymmetrical top has the form

$$H_{sp} + H_{asp} = [(A+C)/2]\,J^2 + [(A-C)/2]\left(J_x^2 + kJ_y^2 - J_z^2\right), \tag{2.2}$$

$$J^2 = J_x^2 + J_y^2 + J_z^2,$$

where

$$A = \frac{3}{16mr^2}\left[1 - \frac{m-m^*}{4m} - \frac{(m-m^*)^2}{2mM}\right]^{-1}, \tag{2.3}$$

$$B = \frac{3}{16mr^2}\left[1 - \frac{m-m^*}{2m}\right]^{-1},$$

$$C = \frac{3}{16mr^3}\left[1 - \frac{3(m-m^*)}{4m} - \frac{(m-m^*)^2}{2mM}\right]^{-1}$$

are the rotational constants depending on the masses m and m^* of the Y and Y* atoms, on the total mass M of the molecule, and on the distance r between the X and Y or X and Y* atoms. The asphericity parameter $(A-C)/(A+C)$ and the asymmetry parameter $k = (2B-A-C)/(A-C)$ are proportional to the small value $(m-m^*)/m$. Therefore, the term $[k(A-C)/2]J_y^2$ in eq. (2.2) may be omitted as it is of second order in $(m-m^*)/m$. The tensor operator $R^{4(4,A_1)}$ for the above chosen orientation of the molecular frame has the form

$$R^{4(4,A_1)} = 4\sqrt{10/3}\left(T_{4,4} + T_{4,-4} + \sqrt{14/5}\,T_{4,0}\right), \tag{2.4}$$

where the rotational tensor operators are *

$$T_{4,\pm 4} = (1/4)J_{\mp}^4,$$

$$T_{4,0} = \left(1/2\sqrt{70}\right)\left(35J_z^4 - 30J^2J_z^2 + 3J^4 + 25J_z^2 - 6J^2\right), \tag{2.5}$$

$$J_{\pm} = J_x \pm iJ_y.$$

For XY^*Y_3 we choose the orientation of the molecular frame so that the z axis lies along the C_3 one. This results in the following rotational hamiltonian:

$$H = AJ^2 + (C-A)J_z^2 + tR^{4(4,A_1)}, \tag{2.6}$$

with the rotational constants

$$A = B = 3/16mr^2,$$

$$C = \frac{3}{16mr^2}\left[1 + \frac{3(m-m^*)}{8m} - \frac{3(m-m^*)^2}{16m(m+m^*)}\right]^{-1}.$$

The asphericity parameter is again proportional to $(m-m^*)/m$. For this coordinate system

$$R^{4(4,A_1)} = \left(16\sqrt{30}/9\right)\left(T_{4,3} - T_{4,-3} + \sqrt{7/10}\,T_{4,0}\right), \tag{2.7}$$

$$T_{4,\pm 3} = \mp\left(1/2\sqrt{2}\right)J_{\mp}^3\left(2J_z \pm 3\right).$$

The hamiltonian (2.6) is invariant with respect to the molecular symmetry group C_{3v}.

A concrete example of the molecule considered

* J_- is a raising operator and J_+ is a lowering one in the molecular frame.

above is CCl_4. Its rotational constant $B \approx 5.7 \times 10^{-2}$ cm^{-1}. The contribution of the aspherical terms for $C^{37}Cl_2{}^{35}Cl_2$ to the rotational energy is two orders smaller since $(A-C)/2 \approx 8.1 \times 10^{-4}$ cm^{-1}. A crude estimation of the constant t in eq. (2.1) for the ground vibrational state is $\approx 10^{-9}$ cm^{-1}. Therefore, the deviations from the rigid asymmetrical top are not important up to $J \approx 100$. At the same time the constant t has to be considerably larger for the vibrational state ν_1 due to $2\nu_2 \approx \nu_1$. If one assumes $t \approx 10^{-6}$ cm^{-1}, the centrifugal distortion effects become of the same order as those of the asphericity at $J \approx 20$. For such moments the effects of the centrifugal distortion due to the sixth-rank operator $R^{6(6,\,A_1)}$ and other high-order operators are still small. Thus, the ground vibrational state of $C^{37}Cl_2{}^{35}Cl_2$ has the rotational structure typical of the asymmetrical top but the rotational structure of the excited ν_1 vibrational state must vary with J from the cluster structure characteristic of the asymmetric top to that determined mainly by the operator $R^{4(4,\,A_1)}$. Another molecule $Os^{18}O_2{}^{16}O_2$ may be more suitable from the point of view of experimental investigations but there are no highly degenerate clusters of the rotational levels of this molecule because the nuclei ^{16}O and ^{18}O have a zero nuclear spin.

Let us consider the structure of the rotational multiplets of the $XY_2^*Y_2$ molecule in more detail. The operator H_{sp} in (2.1) is not essential and the hamiltonian may be written in the following tensor form

$$H = [(A-C)/4]\left(T_{2,2} + T_{2,-2} - \sqrt{6}\,T_{2,0}\right) + 4t\sqrt{10/3}\left(T_{4,4} + T_{4,-4} + \sqrt{14/5}\,T_{4,0}\right), \quad (2.8)$$

$$T_{2,\pm 2} = (1/2)J_{\mp}^2,$$

$$T_{2,0} = \left(1/\sqrt{6}\right)\left(3J_z^2 - J^2\right).$$

The hamiltonian (2.8) is invariant with respect to the group D_2. For $A = C$ it becomes invariant with respect to a much higher cubic symmetry group.

2.1. Harmonic approximation

We use the boson representation proposed by Marshalek [11] for the angular momentum operators in the molecular frame to study the structure of the rotational multiplet. The operators

$$J_z = J - b^+b,$$

$$J_+ = J_-^+ = b^+(2\hat{J} - b^+b)^{1/2},$$

$$\hat{J} = (1/2)a^+a, \quad (2.9)$$

act in the space of wavefunctions

$$|JM'M\rangle = \frac{(a^+)^{2J}(c^+)^{J-M'}}{[(2J)!(J-M')!]^{1/2}}\Phi_{JM}, \quad (2.10)$$

with a fixed projection M' on one of the axes of the laboratory frame. The boson operators a^+ and a (changing the quantum number J), b^+ and b (changing the projection M on the molecular frame), c^+ and c (changing the quantum number M') satisfy the following commutation relations

$$[a, a^+] = [b, b^+] = [c, c^+] = 1,$$

$$[a, b] = [a, b^+] = [a, c] = [a, c^+] = [b, c] = [b, c^+] = 0. \quad (2.11)$$

Further we shall use the operators

$$J_z = J - b^+b,$$

$$J_+ = J_-^+ = b^+(2J - b^+b)^{1/2}, \quad (2.12)$$

acting in the space of wavefunctions Φ_{JM}, corresponding to the states of one rotational multiplet.

Applying the boson expansion method to the hamiltonian (2.8) we shall confine ourselves to the harmonic approximation using the following relations

$$J_z^2 \approx J^2 - (2J-1)b^+b,$$

$$J_z^4 \approx J^4 - (2J-1)(2J^2 - 2J - 1)b^+b,$$

$$J_+ = J_-^+ \approx (2J)^{1/2}b^+,$$

$$J_+J_z^m \approx J^m(2J)^{1/2}b^+,$$

$$J_+^2 = \left(J_-^2\right)^+ \approx [2J(2J-1)]^{1/2}b^+b^+,$$

$$J_+^2J_z^m \approx J^m[2J(2J-1)]^{1/2}b^+b^+. \quad (2.13)$$

These formulae can be obtained by the procedure described in ref. [9]. The general form of the hamiltonian in the harmonic approximation is

$$H = E_J + (P + iQ)b^+b^+ + (P - iQ)bb + Sb^+b, \quad (2.14)$$

where the coefficients E_J, P, Q, S depend on the parameters of the hamiltonian (2.8) and on the quantum number J. The harmonic approximation adequately describes the states with the nearly maximal angular momentum projection M on the rotation axis. In the harmonic approximation M is a "good" quantum number and it may be used to classify levels for a given rotational multiplet which correspond to the precession of J around the stable rotation axis. The energy of these levels,

$$E_{JM} = E_J - (1/2)S + (S/|S|)(S^2 - 4P^2 - 4Q^2)^{1/2} \times (J - |M| + 1/2), \quad (2.15)$$

may be found by the diagonalization of eq. (2.14) (see appendix). The condition $S^2 > 4(P^2 + Q^2)$ is necessary for the states with the energy (2.15) to be stable and the corresponding axis to be that of the stable rotation. The critical value J_0 (for which $S^2 = 4(P^2 + Q^2)$) is the transition point from the states E_{JM} to those corresponding to the precession of J around some other stable rotation axis. The harmonic approximation is not applicable near the critical points J_0. Therefore, it may be used to analyse the stability of any stationary axis but it cannot be used to determine the orientation of other stationary axes. Classical mechanics or an asymptotic approach must be employed for this purpose.

In classical mechanics we write the hamiltonian (2.8) in terms of J_x, J_y, J_z using eq. (2.5) and find the stationary solutions from the equations

$$\dot{J}_x = \{H, J_x\} = 0, \quad \dot{J}_y = \{H, J_y\} = 0, \quad \dot{J}_z = \{H, J_z\} = 0, \quad (2.16)$$

where $\{\ldots\}$ denotes the classical Poisson bracket. The solution of eqs. (2.16) defines the orientation of the stationary rotation axes. The analysis made in the harmonic approximation (see section 3.1) shows that two types of the axes are unstable for any J, one is stable for any J and the stability of the other axes depends on the J value.

2.2. Asymptotic approach (see ref. [5])

The classical equations (2.16) define the orientation of the stationary rotation axes in a zero-order approximation in the small parameter J^{-1}. Let us use the same parameter in the quantum problem. For this purpose we transform the hamiltonian (2.8) by rotating the molecular frame through the Euler angles φ, θ, ψ. The corresponding transformations of the lth-rank tensor operators is

$$R(\varphi, \theta, \psi) T_{lm} R^{-1}(\varphi, \theta, \psi) = \sum_{m'=-l}^{l} D^{(l)}_{m'm}(-\varphi, -\theta, -\psi) T_{lm'}, \quad (2.17)$$

where

$$R(\varphi, \theta, \psi) = \exp(i\psi J_z) \exp(i\theta J_y) \exp(i\varphi J_z) \quad (2.18)$$

is the rotation operator, $D^{(l)}_{mm'}$ is the Wigner function *. The transformed hamiltonian takes the form:

$$\begin{aligned}\tilde{H} &= R(\varphi, \theta, \psi) H R^{-1}(\varphi, \theta, \psi) \\ &= [(A - C)/4] \sum_{m=-2}^{2} \big[D^{(2)}_{m,2}(-\varphi, -\theta, -\psi) \\ &\quad + D^{(2)}_{m,-2}(-\varphi, -\theta, -\psi) \\ &\quad - \sqrt{6}\, D^{(2)}_{m,0}(-\varphi, -\theta, -\psi) \big] T_{2,m} \\ &\quad + 4t\sqrt{10/3} \sum_{m=-4}^{4} \big[D^{(4)}_{m,4}(-\varphi, -\theta, -\psi) \\ &\quad + D^{(4)}_{m,-4}(-\varphi, -\theta, -\psi) \\ &\quad + \sqrt{14/5}\, D^{(4)}_{m,0}(-\varphi, -\theta, -\psi) \big] T_{4,m} \\ &= \sum_m \hat{H}_m(\varphi, \theta, \psi). \end{aligned} \quad (2.19)$$

For the sake of simplicity the transformed hamiltonian is written in terms of the operators $\hat{H}_m$ containing linear combinations of the operators $T_{2,m}$ and $T_{4,m}$. The orientation of new quantization axes (the stationary rotation ones) may be found from the equation

$$\langle J, J-1 | \hat{H}_{-1}(\varphi, \theta, \psi) | J, J \rangle = \langle J, J | \hat{H}_{+1}(\varphi, \theta, \psi) | J, J-1 \rangle = 0. \quad (2.20)$$

* Our definition of the rotation of the molecular frame differs from that of Edmonds, but that of the Wigner function coincides with the latter (see ref. [12]).

Table 1
Stationary rotation axes for the $XY_2^*Y_2$ molecules and the corresponding energy E_J of the state with $|M| = J$

Axis	Axis orientation	Permissible values of parameter δ	Stability region	$4E_J/(A-C)J(2J-1)$
C_2^z	$\varphi = \theta = \psi = 0$	$0 \leqslant \delta \leqslant \infty$	$0 \leqslant \delta < 1$ $\delta > 2$	$-1 + \delta/5$
C_2^y	$\varphi = \theta = \pi/2,\ \psi = 0$	$0 \leqslant \delta \leqslant \infty$	$\delta > 1$	$\delta/5$
C_2^x	$\varphi = \psi = 0,\ \theta = \pi/2$	$0 \leqslant \delta \leqslant \infty$	$0 \leqslant \delta \leqslant \infty$	$1 + \delta/5$
C^{yz}	$\varphi = \pi/2,\ \psi = 0,\ \cos 2\theta = 1/\delta$	$\delta \geqslant 1$	$1 < \delta < 3$	$-1/4 - 1/4\delta - \delta/20$
C^{xz}	$\varphi = \psi = 0,\ \cos 2\theta = 2/\delta$	$\delta \geqslant 2$	–	$-1/\delta - \delta/20$
C^{xy}	$\theta = \pi/2,\ \psi = 0,\ \cos 2\varphi = -1/\delta$	$\delta \geqslant 1$	–	$1/2 - 1/4\delta - \delta/20$
C_3	$\cos 2\varphi = 1/(1-2\delta/3)$, $\cos^2\theta = 1/3 + 1/\delta,\ \psi = 0$	$\delta \geqslant 3$	$\delta > 3$	$-1/\delta - 2\delta/15$

Its solution defining seven types of stationary rotation axes is given in table 1. The orientation of each axis varies with J and depends on the parameter

$$\delta = 16\sqrt{10/3}\,\frac{t}{A-C}(J-1)(2J-3), \qquad (2.21)$$

which is due to the tensor structure of the hamiltonian (2.8) *.

The average value of $\hat{H}_0$ from eq. (2.19) is used as the zero-order approximation for the energy of the rotational levels with the given J

$$E_{JM}^{(0)} = \langle JM|\hat{H}_0(\varphi, \theta, \psi)|JM\rangle. \qquad (2.22)$$

Here M is the angular momentum projection on one of the stable rotation axes whose orientation is defined by the angles φ, θ, ψ.

Formula (2.22) is applicable to states corresponding to the precession of the J vector around the stable rotation axis. It yields a fairly good approximation for levels with such $|M|$ that $(J - |M|) \ll J$ since the condition (2.20) remains valid for these levels with an accuracy up to J^{-1}. This group of levels forms a well-defined cluster structure inside the rotational multiplet. Table 1 presents the energies E_J of the states with the maximal projection $|M| = J$ for all the stationary axes. The approximation (2.22) is not applicable to unstable axes.

Although the asymptotic approximation is very simple it enables one to obtain reasonable numerical estimations for some energy levels as well as to describe the cluster structure of the whole rotational multiplet. Let us consider the rotational multiplet with $J = 20$ for the $XY_2^*Y_2$ molecule ($\delta = 3.423$) as an example. Table 2 shows exact (numerical diagonalization of eq. (2.8)) and approximate energy levels of this multiplet. The cluster structure of the multiplet obtained by the asymptotic approximation (2.22) is rather complicated. It includes four-fold degenerate clusters (C^{yz}, M) and three types of two-fold degenerate clusters (C_2^x, M), (C_2^y, M), (C_2^z, M). The clusters (C_2^z, M) are well defined for the projection $|M| = 20$, 19, 12–8. At $|M| = 20$, 19 the energies of these clusters decrease and at $|M| = 12$–8 they increase as $|M|$ decreases. Actually the clusters (C^{yz}, 20) and (C^{yz}, 19) are formed by splitting the eight-fold degenerate cluster (C_3, 20) since the J value is close to the critical J_B one (see section 3.3). The energy level patterns in the transition regions (see section 3.2) do not correspond to an unambiguous cluster structure. Thus the clusters (C_2^z, 14) and (C_2^z, 13) may be equally classified as the splitted cluster (C^{yz}, 18), and the B_2 level from the cluster (C_2^x, 16) together with the single B_1 level may be treated as the (C_2^z, 7) cluster.

* The condition of zero coefficients before b^+ and b in the transformed hamiltonian (2.19) in the harmonic approximation may be used to find the orientation of the stationary axes. It is easy to show that this condition coincides with that of eq. (2.20).

Table 2
Relative energies of the levels of the $J = 20$ rotational multiplet of the $XY_2^*Y_2$ molecule. $(A-C)/2 = 10^{-3}$ cm^{-1}, $t = 0.3333\ 10^{-6}$ cm^{-1}. The absolute energy of the uppermost level of rotational multiplet equal to 0.657556 cm^{-1} is taken to be unity

Type of cluster	Symmetry	Level energy		
		exact value	asymptotic approximation	harmonic approximation
$(C_2^x, 20)$	A	1.00000	0.9991	0.9999
	B_3	1.00000		
$(C_2^x, 19)$	B_2	0.71062	0.7071	0.7095
	B_1	0.71062		
$(C_2^x, 18)$	A	0.47484	0.4666	0.4190
	B_3	0.47483		
$(C_2^y, 20)$	B_2	0.41170	0.4060	0.4105
	A	0.41164		
$(C_2^x, 17)$	B_1	0.29107	0.2717	0.1286
	B_2	0.28992		
$(C_2^y, 19)$	B_3	0.23024	0.2030	0.2166
	B_1	0.22487		
$(C_2^x, 16)$	A	0.16430	0.1170	−0.1618
	B_3	0.14586		
–	B_2	0.11143	–	–
$(C_2^z, 8)$	A	0.07070	0.1235	–
	B_1	0.05416		
$(C_2^z, 9)$	B_2	−0.00606	0.0375	–
	B_3	−0.01502		
$(C_2^z, 10)$	B_1	−0.08698	−0.0497	–
	A	−0.08847		
$(C_2^z, 11)$	B_3	−0.16387	−0.1353	–
	B_2	−0.16502		
$(C_2^z, 20)$	B_1	−0.18374	−0.1871	−0.1851
	A	−0.18374		
$(C_2^z, 12)$	B_1	−0.23696	−0.2158	–
	A	−0.23699		
$(C_2^z, 19)$	B_2	−0.27738	−0.3011	−0.2951
	B_3	−0.27741		
$(C_2^z, 13)$	B_2	−0.31875	−0.2879	–
	B_3	−0.31881		
$(C_2^z, 14)$	A	−0.33877	−0.3474	–
	B_1	−0.33888		
$(C^{yz}, 19)$	A	−0.41073	−0.3548	−0.4623
	B_1	−0.41073		
	B_2	−0.41381		
	B_3	−0.41381		
$(C^{yz}, 20)$	A	−0.47261	−0.4414	
	B_1	−0.47261		
	B_2	−0.47285		
	B_3	−0.47285		

3. Rearrangement of rotational structure of isotopic modifications of molecule XY_4 under excitation of states with high J

Let us consider the rotational structure of an isolated vibrational state of the $XY_2^*Y_2$ molecule. The rotational multiplets with $J \gg 1$ are of primary interest to us. The multiplet structure is to change (as follows from the hamiltonian (2.8)), provided parameters satisfy the condition $(A - C) \approx tJ^2$ (i.e. $\delta \approx 1$). The approximate expressions for the energy E_J of the levels with the maximal projection on the stationary axes obtained in section 2 enable one to describe the qualitative changes of the multiplet structure. Fig. 1 shows the E_J dependence on the parameter δ (eq. (2.21)). Let us use the harmonic approximation to determine more precisely the positions of clusters with nearly maximal porjections and to define the stability of the specific axes.

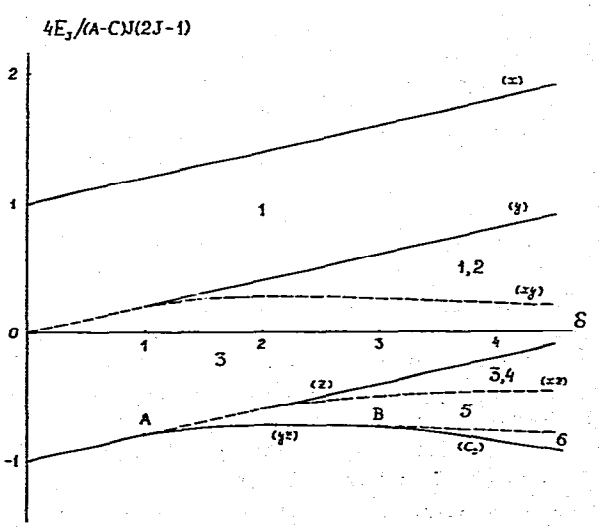

Fig. 1. Relative positions of the extreme clusters (solid lines) and the transition regions (dotted lines) in the system of rotational levels of the $XY_2^*Y_2$ molecule. Indices in parentheses denote the axis of rotation.

Table 3
Hamiltonian (2.8) in the harmonic approximation

Precession around C_2^z axis
$P=(1/8)(A-C)[2J(2J-1)]^{1/2}$, $Q=0$, $S=(1/2)(A-C)(2J-1)(3/2-\delta)$ $\omega_z=[(\delta_1-\delta)(\delta_2-\delta)]^{1/2}$, $\delta_{1,2}=(1/2)\{3\pm[2J/(2J-1)]^{1/2}\}$ $0\leqslant\delta<1$: $E_{JM}=(1/2)(2J-1)(A-C)[-(J+5)(5-\delta)/10+7/4+\omega_z(J-\lvert M\rvert+1/2)]$ $2<\delta<\infty$: $E_{JM}=(1/2)(2J-1)(A-C)[-(J+5)(5-\delta)/10+7/4-\omega_z(J-\lvert M\rvert+1/2)]$
Precession around C_2^y, $\delta>1$
$P=(1/4)(A-C)[2J(2J-1)]^{1/2}$, $Q=0$, $S=-(1/2)(A-C)\delta(2J-1)$ $\omega_y=(\delta^2-\delta_3^2)^{1/2}$, $\delta_3=[2J/(2J-1)]^{1/2}$ $E_{JM}=(1/2)(A-C)(2J-1)[\delta(J+5)/10-\omega_y(J-\lvert M\rvert+1/2)]$
Precession around C_2^x
$P=-(1/8)(A-C)[2J(2J-1)]^{1/2}$, $Q=0$, $S=-(A-C)(2J-1)(3/2+\delta)$ $\omega_x=[(\delta+\delta_1)(\delta+\delta_2)]^{1/2}$ $E_{JM}=(1/2)(A-C)(2J-1)[(J+5)(5+\delta)/10-7/4-\omega_x(J-\lvert M\rvert+1/2)]$
Precession around C^{yz}, $1<\delta<3$
$P=-(A-C)(1/16\delta)(3\delta^2-3\delta-2)[2J(2J-1)]^{1/2}$, $Q=0$ $S=(A-C)(1/8\delta)(\delta^2+3\delta-2)(2J-1)$ $\omega_{yz}=(1/4\delta)[(\delta^2+3\delta-2)^2-\delta_3^2(3\delta^2-3\delta-2)^2]^{1/2}$ $E_{JM}=(1/2)(A-C)(2J-1)[-(J+5)(1/40\delta)(\delta^2+10\delta+5)$ $+7(\delta+1)/8\delta+\omega_{yz}(J-\lvert M\rvert+1/2)]$
Precession around C_3 axes, $\delta>3$
$P=(1/4)(A-C)(1-\cos 2\varphi-2/\delta)[2J(2J-1)]^{1/2}$ $Q=(1/4)(A-C)\cos\theta\sin 2\varphi[2J(2J-1)]^{1/2}$ $S=(A-C)(2J-1)(\delta/3-1/\delta)$ $\omega_{C_3}=(2/3\delta)[(\delta^2-3)^2-3\delta_3^2(\delta^2+3)]^{1/2}$ $E_{JM}=(1/2)(A-C)(2J-1)[-(J+5)(\delta/15+1/2\delta)$ $+7/2\delta+\omega_{C_3}(J-\lvert M\rvert+1/2)]$

3.1. Cluster structure of multiplet in harmonic approximation

The harmonic approximation is valid for the precession of the angular momentum vector J around the stable rotation axis. In contrast to the asymptotic approximation the harmonic one for the hamiltonian (2.19) takes into account $\hat{H}_0$ and $\hat{H}_{\pm 2}$ in the linear approximation over the $(J-|M|)$ value. The harmonic approximation yields accurate energies for some clusters with a nearly maximal $|M|$. The energy levels forming each cluster are strictly degenerate in the zero-order harmonic approximation. Nevertheless, a reasonable estimate of the splitting of levels inside a cluster may be obtained using a properly symmetrized wavefunction of the harmonic approximation (see section 3.4, eqs. (3.15)).

The results of the application of the harmonic approximation to the hamiltonian (2.8) are given in table 3.

The harmonic approximation yields more accurate results than the asymptotic one for those states which correspond to the precession of J with a nearly maximal projection. Otherwise, the asymptotic approximation is better for the clusters with $|M|$ significantly different from J (see the comparison between the exact and approximate calculations in table 2 and fig. 2). Both methods use the smallness of the matrix elements of the

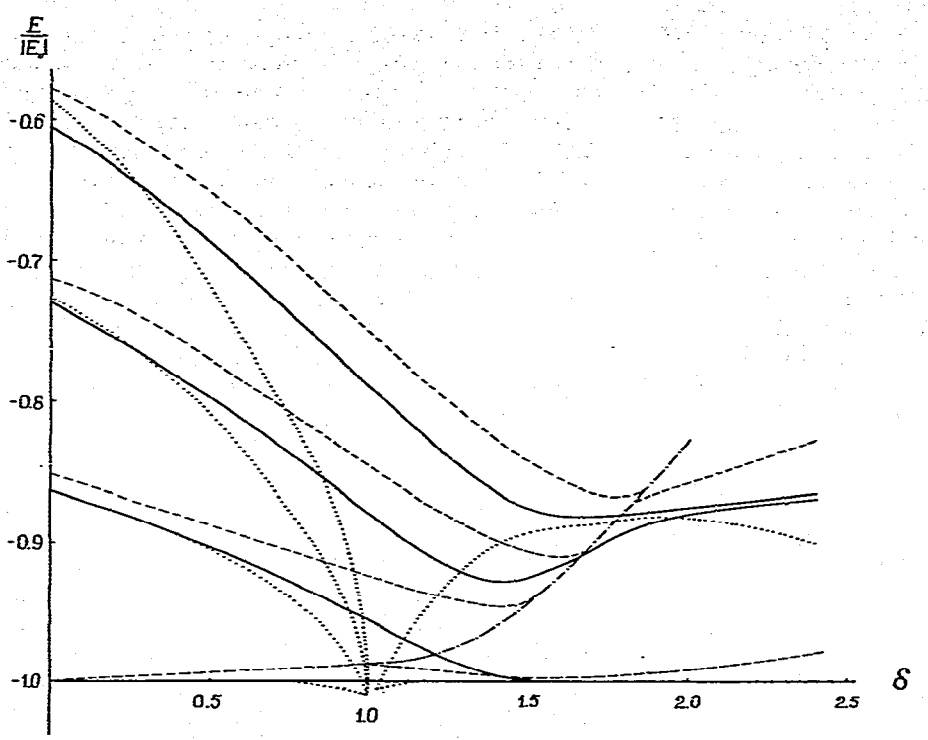

Fig. 2. The dependence of the lower energy levels on δ for the $J = 20$ rotational multiplet of the $XY_2^*Y_2$ molecule in the vicinity of the critical point A. The energy E_1 of the lowest energy level is taken to be unity. ———: The exact numerical solution for the hamiltonian (2.8). — — —: The asymptotic approximation of eq. (2.22). ....: The harmonic approximation (see table 3). –·–·–: The energy corresponding to the unstable rotation axis C^{yz} (see table 1). The doublet splitting is not shown.

hamiltonian (2.19) with $|\Delta M| \geq 3$. The asymptotic approximation additionally assumes that the matrix elements with $\Delta M = \pm 2$ are small. There is no such limitation in the harmonic approximation but the diagonal matrix elements of the hamiltonian (2.19) are taken into account only in the linear over $(J - |M|)$ approximation. Further improvement may be achieved by using three-term recurrence relations [13]. This approach enables one to take into consideration diagonal and non-diagonal (with $\Delta M = \pm 2$) matrix elements of the hamiltonian (2.19). The harmonic approximation is valid in a wide range of the parameter δ. Nevertheless, it is inapplicable in the transition regions, i.e. close to the critical points A and B (fig. 1) and those where the C_2^y and C_2^z axes become stable ($\delta = 1$, 2). Therefore, the regions of the stable precession around the C_2^z ($0 \leqslant \delta < 1 - 1/8J$), C^{yz} ($1 + 1/4J < \delta < 3 + 1/12J$) and C_3 ($\delta > 3 + 1/3J$) axes are separated on δ by an interval of order J^{-1}. Indeed, all the energy levels of the given rotational multiplet vary continuously with J. The width of the transition region on the δ line, where the harmonic approximation is a fortiori inapplicable, was shown to be of order $J^{-2/3}$ [14]. The harmonic approximation works much worse for the clusters (C^{yz}, M) and (C_3, M) than for ($C_2^{x,y,z}$, M) since the equivalent axes bring about a stronger intra-cluster splitting.

3.2. *Modification of multiplet cluster structure under excitation of states with high J*

The analysis of the multiplet cluster structure performed in sections 2.2 and 3.1 as well as results of the numerical calculations show that the rota-

tional multiplets with small J (small δ) possess the rotational structure typical of an asymmetric top. This top is characterized by two stable rotation axes for maximal and minimal moments of inertia and by an unstable one for intermediate moments of inertia. The increase of the quantum number J results in new stable rotation axes and in the change of the stability of the old ones. Only the C_2^x axis corresponding to the minimal moment of inertia remains unchanged. The states with the maximal projection $|M| = J$ on the stable rotation axis (the solid lines in fig. 1) form the extreme clusters. The clusters with smaller $|M|$ are positioned below (for the axes C_2^z, $\delta > 2$; C_2^y, C_2^x) or above (for the axes C_2^z, $0 \leqslant \delta < 1$; C^{yz}, C_3) the extreme one. The energy levels close to the energy of states with the projection $|M| = J$ on the unstable axis (the dotted line in fig. 1) form the transition region between the clusters of different types. The dotted line is a border for the clusters of a given type since the orientation of the unstable axis corresponds to the saddle point of the rotational energy surface. The dotted line corresponding to the unstable axis C^{yz} in fig. 1 is a border separating the (C_3, M) and (C^{yz}, M) clusters. The dotted line corresponding to the C_2^z($1 < \delta < 2$) and C^{xz} unstable axes separates the (C^{yz}, M) and (C_2^z, M) clusters. Finally, the dotted line corresponding to the C_2^y($0 \leqslant \delta < 1$) and C^{xy} axes separates the (C_2^y, M) clusters from the (C_2^x, M) ones.

As shown earlier, six types of stable rotation axes (see table 1) may exist in the $XY_2^*Y_2$ molecule for different J (or δ). Thus, the six types of clusters are present in the rotational multiplets of this molecule. Six regions in the (E, δ) coordinates are shown in fig. 1 corresponding to the existence of different types of clusters:

(1) Two-fold degenerate clusters (C_2^x, M).
(2) Two-fold degenerate clusters (C_2^y, M).
(3) Two-fold degenerate clusters (C_2^z, M).
(4) Two-fold degenerate clusters (C_2^z, M).
(5) Four-fold degenerate clusters (C^{yz}, M).
(6) Eight-fold degenerate clusters (C_3, M).

The C_2^z axis and the corresponding clusters are listed twice because there are two unlinked stability intervals over δ which correspond to regions 3 and 4 in fig. 1. Regions 3 and 4 partly overlap each other and both types of clusters are present in the overlapping part of these regions. There are also two types of (C_2^x, M) and (C_2^y, M) clusters present in the overlapping part of regions 1 and 2 due to the stability of both the non-equivalent C_2^y and C_2^x axes for the corresponding δ values.

Sometimes, the states with $|M| < J$ are better described by the precession approximation than those with the maximal projection on the same axis due to the local instability of that very axis. A general tendency arises for the $XY_2^*Y_2$ molecules: there appear higher-degenerate clusters with the increase of the quantum number J.

3.3. Critical points

We now consider in detail the critical region (close to the points A and B) on the curve representing the dependence of the extreme cluster energy on the parameter δ (see fig. 1). Our aim is to explain the abovementioned regular tendency in the change of the cluster structure of the multiplet. The precession frequency vanishes at the critical point. This means that the precession changes qualitatively upon passing through this point. Indeed, we have seen earlier (section 3.1) that to the left of the point A the J vector precesses around the C_2^z axis whereas to the right of the point A it may precess around any of the two equivalent C^{yz} axes. The true motion of the J vector is, naturally, the superposition of these precessions. Symmetrized wavefunctions have to be used, correspondingly, in the quantum problem. The same character of the J vector motion is observed to be left of the point B. To the right of it each of the two C^{yz} axes transforms into an axis of the C_3 type. Finally, we have four axes around which the J vector may precess independently and its true motion is their appropriate superposition. Thus, the number of stable axes doubles at the points A and B and the degeneracy of the respective clusters doubles as well.

Now consider the transition region in the classical limit in more detail. We use the hamiltonian (2.8) and write the rotational energy dependence on the angles θ and φ as

$$E(\theta, \varphi) = (1/2)(A - C)J^2\epsilon(\theta, \varphi), \qquad (3.1)$$

$$\epsilon(\theta, \varphi) = \sin^2\theta\cos^2\varphi - \cos^2\theta + (\delta/2) \times \left[\cos^4\theta + \sin^4\theta(\cos^4\varphi + \sin^4\varphi) - 3/5\right].$$

θ and φ define the orientation of the angular momentum vector J in the molecular frame, i.e. the orientation of the axis of molecular rotation. The minimum of the function $\epsilon(\theta, \varphi)$ corresponds to the orientation of the stable rotation axis.

To study the critical region close to the point A, we expand $\epsilon(\theta, \varphi)$ in a series over θ near $\theta = 0$ up to terms proportional to θ^4

$$\epsilon(\theta, \varphi) = \epsilon_0(J) + \left(1 - J^2/J_A^2 + \cos^2\varphi\right)\theta^2 + \left[7/8 - (1/3)\cos^2\varphi + (1/8)\cos^4\varphi\right]\theta^4, \quad (3.2)$$

where

$$E_0(J) = (1/2)(A - C)J^2\epsilon_0(J) = (1/2)(A - C)J^2\left(J^2/5J_A^2 - 1\right) \quad (3.3)$$

is the energy of the molecular rotation around the C_2^z axis. $J_A^2 = \sqrt{3}\,(A - C)/32\sqrt{10}\,t$ is the critical value of the angular momentum at the point A. For $J < J_A$, $\theta = 0$ is the minimum of the function (3.2) and the expression (3.3) gives the energy of the lowest-energy level of the multiplet with an accuracy of order J^{-1}. For $J > J_A$, $\theta = 0$ becomes a saddle point and the minima correspond to two orientations of the rotation axes $(\theta_0, \pi/2)$ and $(\theta_0, 3\pi/2)$, with $\theta_0 = [(J^2/J_A^2 - 1)/2]^{1/2}$, and

$$E(J) = E_0(J) - (1/8)(A - C)J^2\left(J^2/J_A^2 - 1\right)^2. \quad (3.4)$$

It follows from eqs. (3.3) and (3.4) that the first derivative dE/dJ is continuous whereas the second one d^2E/dJ^2 has a discontinuity at $J = J_A$ with a jump equal to $(A - C)$.

The change in character of the rotational motion may be visualized by the classical trajectories $\epsilon(\theta, \varphi) = \epsilon$ at both sides of the critical point A. Fig. 3 shows the classical trajectories of the top of the J vector around the north pole of a sphere of radius J. The existence of the symmetry axes C_2^x and C_2^y implies that absolutely the same trajectories are positioned close to the south pole of the sphere. In the case of $J < J_A$ these trajectories

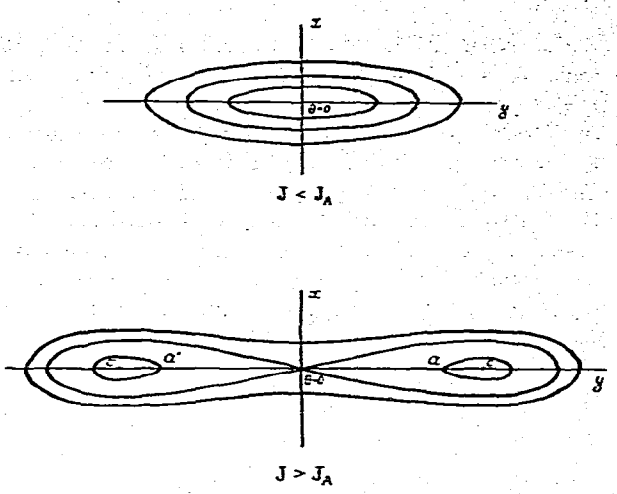

Fig. 3. Classical trajectories in the vicinity of the critical point A.

form a set of curves closed around $\theta = 0$ and stretched in the direction of the y axis. The stretching of these curves increases as J approaches J_A. For $J > J_A$ the pattern of the classical trajectories abruptly changes. Three sets of closed curves are formed instead of one. Two of them are local sets centered at $(\theta_0, \pi/2)$ and $(\theta_0, 3\pi/2)$ (the points c and c′ in fig. 3). The third set is a global one embracing these points as well as the north pole. The three sets are separated from each other by a separatrix, i.e. a trajectory with energy $\epsilon = \epsilon_0$ passing through the saddle point. The separatrix separates the local trajectories from global ones.

We now expand $\epsilon(\theta, \varphi)$ in the critical region close to the point B. We use the expansion near one of the four equivalent axes orientations specified by the angles $(\theta_0 = (1/2)\arccos(1/\delta), \varphi_0 = \pi/2)$. Assuming ν and ϕ to be the deviations from θ_0 and φ_0 we have

$$\epsilon(\nu, \phi) = \tilde{\epsilon}_0(J) + (8/3)\nu^2 + (1/2)\left(1 - J^2/J_B^2\right)\phi^2 - (2\sqrt{2}/3)\nu\phi^2 + (1/3)\phi^4, \quad (3.5)$$

where

$$\tilde{E}_0(J) = (1/2)(A - C)J^2\tilde{\epsilon}_0(J) = -(1/6)(A - C)J_B^2\left(1 + 6J^4/5J_B^4\right) \quad (3.6)$$

is the energy of the rotation around the considered axis, $J_B^2 = \sqrt{27}(A-C)/32\sqrt{10}\,t$ is the critical angular momentum at the point B. For $J > J_B$ the minimum $\epsilon(0, 0)$ of the function (3.5) corresponds to the orientation of the C^{yz} axis and to the energy (3.6). For $J > J_B$ this minimum is transformed into the saddle point and the two equivalent axes become stable ones whose orientation is defined by the angles $\theta = (1/2)\arccos(1/\delta) + \nu_0$, $\varphi = \pi/2 \pm \phi_0$ (the points d and d′ in fig. 4) where $\phi_0 = (J^2/J_B^2 - 1)^{1/2}$, $\nu_0 = (1/4\sqrt{2})\phi_0^2$, and

$$E(J) = \tilde{E}_0(J) - (1/8)(A-C)J^2\left(J^2/J_B^2 - 1\right)^2. \tag{3.7}$$

The comparison between the energies (3.6) and (3.7) defined for both sides of the critical point shows that the first derivative dE/dJ is continuous but the second one, d^2E/dJ^2, has a discontinuity with a jump equal to $(A-C)$.

The classical trajectories for the transition region close to the point B are shown in fig. 4. The character of the motion of J near the critical points A and B is similar. The main difference is that for point B there are two sets of trajectories mirror-symmetrical with respect to the zx plane.

A complete description of the transition region for the quantum problem may be made employing the method proposed in ref. [14], in which a similar transition was investigated for a model many-particle system. The main features of the quantum description of the transitions mentioned above are the following. The independent precession of the vector J around the equivalent axes is impossible in quantum mechanics due to tunelling through the potential barrier separating the two equilibrium positions c and c′ (fig. 3) or d and d′ (fig. 4). This tunnelling leads to the splitting of clusters formed by states with the same projection M on the equivalent axes. This splitting is maximal in the transition region where the barrier is narrow while the turning points a and a′ are close to each other and decreases as J increases. To the left of the transition point the splitted levels smoothly transform into states with different projections on some other rotation axis (see fig. 2).

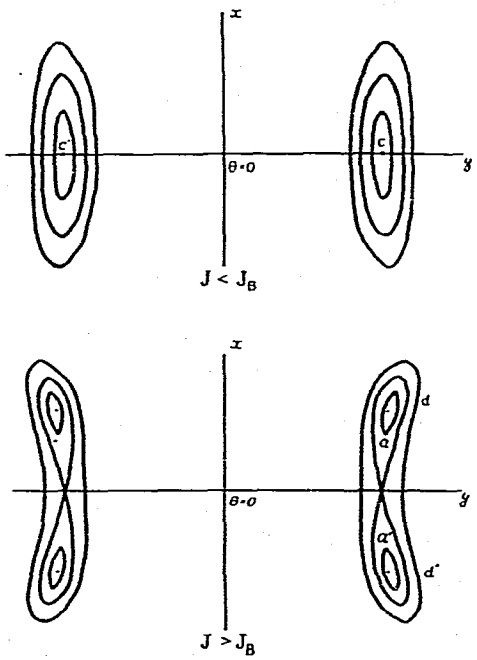

Fig. 4. Classical trajectories in the vicinity of the critical point B.

3.4. Intensities of rovibrational transitions

Up to now we have considered only the rearrangement of the energy levels of the rotational multiplet due to the axis shifting. We now study the effect of axis shifting on the intensities of electromagnetic rovibrational transitions between non-degenerate vibrational states. Rovibrational transitions in the ν_i band of tetrahedral molecules are forbidden in the dipole approximation. But they may be studied by Raman scattering or by more complicated many-quantum processes. For example, recently the CARS technique has been widely employed to obtain high-resolution spectra of the Q-branches of the ν_1 bands for a number of tetrahedral molecules [15].

The intensity of the Raman scattering is defined by the matrix element

$$\langle v, JM'n|\hat{\alpha}|v', JM'n'\rangle \tag{3.8}$$

from the polarization $\hat{\alpha}$ between the levels of two rotational multiplets characterized by the quantum

numbers $vJM'n$ and $v'JM'n'$ (where M' is the angular momentum projection on the laboratory fixed frame, v, v' are the vibrational quantum numbers). The polarization $\hat{\alpha}$ depends on the vibrational coordinates only. Effective rotational hamiltonians have to be usually used in applications which may be obtained by a partial diagonalization of the complete molecular rovibrational hamiltonian. These effective hamiltonians are different for different vibrational states. The corresponding transformation results in the transformed operator

$$\tilde{\hat{\alpha}} = \sum_{\Omega=0}^{\infty} C_\Omega \hat{\alpha}_\Omega, \tag{3.9}$$

where $\hat{\alpha}_\Omega$ depends on the angular momentum operators J_i with the total degree equal to 2Ω.

A characteristic quantity in transition to effective hamiltonians is the Born–Oppenheimer parameter $\kappa = (m_e/m)^{1/4}$ where m_e is the electron mass. The coefficients C_Ω in eq. (3.9) may be presented as $C_\Omega \propto \kappa^{4\Omega}$.

Transitions between the levels of the rotational multiplets belonging to different vibrational states of the $XY_2^*Y_2$ molecule may occur either without or with some change in orientation of the precession axis. In the first case the operator $\hat{\alpha}_0$ makes the main contribution to the sum (3.9) and all other terms may be omitted. Generally, all terms of eq. (3.9) are important for transitions with a change in orientation of the precession axis. Now let us consider the first term in eq. (3.9). The corresponding matrix element (3.8) is factorized and the transition intensity becomes proportional to

$$\Theta_J(n, n') = |\langle JM'n|JM'n'\rangle|^2, \tag{3.10}$$

The factor $\Theta_J(n, n')$ describes the overlap of the rotational wavefunctions (2.10) with the quantum numbers n and n' corresponding to different orientations of the precession axis.

We use the function Φ_{Jn} in the harmonic approximation to calculate the overlap integral Θ_J. For the sake of simplicity we consider only states with the maximal projection $M = J$ on the precession axis. According to (3.10) we introduce the factor

$$\Theta_J^{(i,k)}(\delta, \delta') = \left| \int_{-\infty}^{\infty} \Phi_{JJ}^{(i)*}(\delta, q) \Phi_{JJ}^{(k)}(\delta', q) \mathrm{d}q \right|^2, \tag{3.11}$$

where the function $\Phi_{JJ}^{(i)}(\delta, q)$ for the ground vibrational state corresponds to the precession of J around the axis i ($i = C_2^x, C_2^z$) and the function $\Phi_{JJ}^{(k)}(\delta', q)$ for the vibrational state ν_1 corresponds to the precession around one of the six stable rotation axes listed in table 1. The functions belonging to the upper and lower multiplets have different values of the parameter δ in accordance with section 2.

Table 4
Eigenfunction of different states of the multiplet corresponding to the vector J precession around stable axes. The angles θ, φ are listed in table 1

Axis	Stability	Eigenfunction $\Phi_{JJ}^{(i)}(q)$	$f(\delta)$
C_2^z	$0 \leqslant \delta < 1$, $\delta > 2$	$(f/\pi)^{1/4}\exp(-fq^2/2)$	$[(\delta-\delta_1)/(\delta-\delta_2)]^{1/2}$
C_2^x	$\delta > 1$	$(f/\pi)^{1/4}\exp(-fq^2/2+\mathrm{i}\pi J^{1/2}q/2)$	$[(\delta-\delta_3)/(\delta+\delta_3)]^{1/2}$
C_2^s	$0 \leqslant \delta \leqslant \infty$	$(f/\pi)^{1/4}\exp[-f(q+\pi J^{1/2}/2)^2/2]$	$[(\delta+\delta_1)/(\delta+\delta_2)]^{1/2}$
C^{yz}	$1 < \delta < 2$	$(f/\pi)^{1/4}\exp(-fq^2/2+\mathrm{i}\theta J^{1/2}q)$	$\left[\dfrac{\delta^2+3\delta-2-\delta_3(3\delta^2-3\delta-2)}{\delta^2+3\delta-2+\delta_3(3\delta^2-3\delta-2)}\right]^{1/2}$
C_3	$\delta > 3$	$(f/\pi)^{1/4}\exp[-(f+\mathrm{i}g)(q+\theta J^{1/2})^2/2-\mathrm{i}\varphi J]$ [a]	$\dfrac{(2\delta-3)\left[(\delta^2-3)^2-3\delta_3^2(\delta^2+3)\right]^{1/2}}{(2\delta-3)(\delta^2-3)-3\delta_3(\delta^2-2\delta+3)}$

[a] This function has a non-zero value of $g(\delta) = \dfrac{(1/2)\delta\delta_3[3(\delta^2-9)]^{1/2}}{(2\delta-3)(\delta^2-3)-3\delta_3(\delta^2-2\delta+3)}$.

Table 4 gives the functions Φ_{JJ} describing the precession of J around each of the six stable rotation axes. These functions are obtained by transforming the function (A.11) by the molecular frame rotation described in section 2.2. The explicit form of the rotational functions enables one to easily calculate any of the 12 overlap integrals. Given below are the formulae for some of them. The overlap integrals for which the precession axes are mutually orthogonal have the form

$$\Theta_J^{(z,x)}(\delta,\delta') = \left[\frac{1}{2}\left(\frac{f_z(\delta)}{f_x(\delta')}\right)^{1/2} + \frac{1}{2}\left(\frac{f_x(\delta')}{f_z(\delta)}\right)^{1/2}\right]^{-1} \times \exp\left(-\frac{\pi^2}{4}\frac{f_z(\delta)f_x(\delta')}{f_z(\delta)+f_x(\delta')}J\right),$$

$$\Theta_J^{(z,y)}(\delta,\delta') = \left[\frac{1}{2}\left(\frac{f_z(\delta)}{f_y(\delta')}\right)^{1/2} + \frac{1}{2}\left(\frac{f_y(\delta')}{f_z(\delta)}\right)^{1/2}\right]^{-1} \times \exp\left(-\frac{\pi^2}{4}\frac{J}{f_z(\delta)+f_y(\delta')}\right),$$

$$\Theta_J^{(x,y)}(\delta,\delta') = \left[\frac{1}{2}\left(\frac{f_x(\delta)}{f_y(\delta')}\right)^{1/2} + \frac{1}{2}\left(\frac{f_y(\delta')}{f_x(\delta)}\right)^{1/2}\right]^{-1} \times \exp\left(-\frac{\pi^2}{4}\frac{1+f_x(\delta)f_y(\delta')}{f_x(\delta)+f_y(\delta')}J\right). \quad (3.12)$$

These and all other overlap integrals with different precession axes decrease as $\exp(-aJ)$, $a \approx 1$, with increasing J. For the overlap integrals the coefficient a may be reduced to zero for the cluster (C^{yz}, J) or (C_3, J) in the vicinity of the critical point A or B. For example, the overlap integral

$$\Theta_J^{(z,yz)}(\delta,\delta') = \left[\frac{1}{2}\left(\frac{f_z(\delta)}{f_{yz}(\delta')}\right)^{1/2} + \frac{1}{2}\left(\frac{f_{yz}(\delta')}{f_z(\delta)}\right)^{1/2}\right]^{-1} \times \exp\left(-\frac{J}{4}\frac{[\arccos(1/\delta')]^2}{f_z(\delta)+f_{yz}(\delta')}\right) \quad (3.13)$$

increases for $\delta' \to 1$ (the critical point A). The overlap integrals of the wavefunctions of the same type of rotational clusters belonging to different vibrational states are not exponentially small since their precession axes coincide. For $i=k$ expression (3.11) is reduced to

$$\Theta_J^{(i,i)}(\delta,\delta') = \left[\frac{1}{2}\left(\frac{f_i(\delta)}{f_i(\delta')}\right)^{1/2} + \frac{1}{2}\left(\frac{f_i(\delta')}{f_i(\delta)}\right)^{1/2}\right]^{-1}. \quad (3.14)$$

We compare the overlap integrals calculated from eq. (3.10) with the exact numerical functions of the hamiltonian (2.8) (the parameters $(A-C)/2 = 10^{-3}$ cm^{-1}; $t=0$ in the lower multiplet and $t = 0.55\times10^{-6}$ cm^{-1} ($\delta = 1.23$) in the upper multiplet) with the corresponding integrals calculated with the rotational functions taken in the harmonic approximation. For this purpose we construct a wavefunction of a definite type of symmetry in the harmonic approximation.

The required function for the two-fold degenerate clusters (C_2^x, J) and (C_2^z, J) has the form

$$\Phi_{JJ_0}^{(i)}(q) = (2+\sigma 2S)^{-1/2} \times \left(\Phi_{JJ}^{(i)} + \sigma\Phi_{J-J}^{(i)}\right), \quad i = x, z. \quad (3.15)$$

where S is the non-orthogonality integral and $\sigma = \pm 1$ depending on the symmetry of the function. The overlap integrals for the states of A-type symmetry calculated using the approximate functions for $J=10$ are:

$$\Theta_{10}^{(z,x)}(0, 1.23) = 0.95\times10^{-7},$$

$$\Theta_{10}^{(x,x)}(0, 1.23) = 0.9966.$$

The exact values of the corresponding overlap integrals $\Theta_J(n, n')$ are:

$$\Theta_{10}(1, 6) = 3.0\times10^{-7},$$

$$\Theta_{10}(6, 6) = 0.9975.$$

We now consider the next terms in the transition operator (3.9). The matrix element of the operator $\tilde{\alpha}_1$ for states corresponding to different precession axes is also exponentially small. Since $C_1 \propto \kappa^4$, the contribution of the second term of the sum (3.9) to the transition intensity may be ne-

glected. As Ω increases, the exponential factor grows gradually whereas the pre-exponential decreases proportional to $\kappa^{4\Omega}$. The maximal contribution should be made by those terms (3.9) for which Ω is comparable with the effective difference between the projections of the angular momentum of the initial and final states on the z axis of the molecular frame. If the orientation of the precession axes for these two states differs by an angle θ and each state has a maximal projection on the quantization axis, $2\Omega \approx \Delta M \approx J(1 - \cos\theta) \approx J$. From this it immediately follows that $\kappa^{4\Omega} J^2 \propto \exp[-J \ln(1/\kappa)]$, if $J \propto 1/\kappa$. Thus the contribution of the terms of eq. (3.9) with $\Omega \geqslant 1$ does not change the estimate of the transition intensity calculated by taking into account only the operator $\hat{\alpha}_0$. This implies that a new approximate selection rule is valid for rovibrational transitions with a sufficiently high J value. This selection rule is due to the different orientation of the rotation axes in the molecular frame.

4. Conclusion

The detailed investigation of the rotational states given in the present paper enables us to treat a general scheme for the analysis of critical phenomena in isolated quantum systems with a small number of degrees of freedom rather than simply to find rotational energy levels for one concrete example of nearly spherical tops. The hamiltonian (2.6) for the XY_3Y^* molecule may be treated in the same way as that of eq. (2.8). The results are qualitatively different due to the symmetry difference for eqs. (2.6) and (2.8). The hamiltonian (2.6) possesses, for example, two-fold and six-fold degenerate clusters in the rotational multiplet rather than four-fold and eight-fold ones as the operator (2.8) does. The six-fold degenerate clusters correspond to the orientation of the stable rotation axes in the molecular symmetry planes (the C_{3v} molecular symmetry group). The hamiltonian (2.6) has critical points of a new type. At the same time the critical phenomena themselves are characteristic not only of both types of aspherical tops ($XY_2Y_2^*$ and XY_3Y^*), but also of a wide class of other molecules.

The possibility of a unified treatment of the abovementioned problems and much wider rovibronic problems is due to the fact that the critical phenomena are completely defined by the type of singularity responsible for its appearance. The critical phenomena play an important part in various fields of science and technology investigating any considerably non-linear systems. As yet the critical behaviour has not been treated systematically for isolated molecules.

The experimental investigation of the effects mentioned in this paper may be realized for CCl_4 or OsO_4 with asymmetrical isotopic substitution of Cl or O. Recent experimental studies of high-resolution spectra of $C^{35}Cl_4$ [16] allows one to hope that other isotopic modifications of this molecule would be studied in near future.

Appendix. Diagonalization of the hamiltonian in the harmonic approximation

Let us make a linear canonical transformation of the hamiltonian (2.14) with new boson operators β^+ and β

$$b = u\beta + v\beta^+, \quad b^+ = u^*\beta^+ + v^*\beta. \tag{A.1}$$

β^+ and β satisfy the standard commutation relations

$$[\beta^+, \beta] = 1, \quad [\beta, \beta] = [\beta^+, \beta^+] = 0. \tag{A.2}$$

We demand the coefficients before $\beta^+\beta^+$ and $\beta\beta$ in the transformed hamiltonian to be zero. These two conditions, together with the relations (A.2), may be written in the form of a system of the algebraic equations

$$\begin{aligned} &2P(|u|^2 + |v|^2) + S(uv + u^*v^*) = 0, \\ &2iQ(|u|^2 + |v|^2) + S(uv - u^*v^*) = 0, \\ &|u|^2 - |v|^2 = 1, \end{aligned} \tag{A.3}$$

defining the coefficients of the transformation (A.1).

We take the coefficients u and v in the form

$$u = e^{i\alpha}\mathrm{ch}\eta, \quad v = e^{i\beta}\mathrm{sh}\eta. \tag{A.4}$$

Substitution of eq. (A.4) into eq. (A.3) yields

the following solutions

$$u=\left[\frac{1}{2}\left(\frac{|S|}{(S^2-4P^2-4Q^2)^{1/2}}+1\right)\right]^{1/2}e^{i\alpha},$$

$$v=\frac{|S|}{S}\left[\frac{1}{2}\left(\frac{|S|}{(S^2-4P^2-4Q^2)^{1/2}}-1\right)\right]^{1/2}e^{i\beta},$$

$$\mathrm{tg}(\alpha+\beta)=Q/P, \qquad (A.5)$$

which enable one to represent the hamiltonian in the boson approximation in the form of eq. (2.15).

We now express the wavefunction Φ_{JM} for the hamiltonian (2.15) for the lowest state with the projection $M=J$ through the vacuum function $|0\rangle$ for the boson operators b^+ and b. The function Φ_{JJ} satisfies the equation

$$\beta\Phi_{JJ}=(u^*b-vb^+)\Phi_{JJ}=0. \qquad (A.6)$$

It can easily be verified that the normalized solution of eq. (A.6) has the form

$$\Phi_{JJ}=(|u|)^{-1/2}\exp\left(\frac{v}{2u^*}b^+b^+\right)|0\rangle. \qquad (A.7)$$

The function (A.7) allows one to easily calculate the matrix elements of the operators containing the boson operators b^+ and b for the states corresponding to the precession around a given axis.

The coordinate representation proves to be useful for calculating overlap integrals of wavefunctions corresponding to the vector J precession around differently oriented axes. For this purpose we introduce a dimensionless coordinate q by the relation

$$b^+=(1/\sqrt{2})(q-\mathrm{d}/\mathrm{d}q),$$

$$b=(1/\sqrt{2})(q+\mathrm{d}/\mathrm{d}q). \qquad (A.8)$$

We put (A.8) into the equation $H\Phi_{JM}=E\Phi_{JM}$ with the hamiltonian (2.14) and transform the so-obtained equation by the substitution

$$\Phi_{JM}(q)=\Psi(q)\exp\left(-i\frac{Q}{S-2P}q^2\right) \qquad (A.9)$$

to the form

$$-\frac{S-2P}{2}\frac{\mathrm{d}^2\Psi}{\mathrm{d}q^2}+\frac{S^2-4P^2-4Q^2}{2(S-2P)}q^2\Psi$$
$$=(E-E_0+S/2)\Psi. \qquad (A.10)$$

Eq. (A.10) can describe small precessions near equilibrium, $q=0$, if $(S+2P)$ and $(S-2P)$ have the same sign and $S^2-4P^2>4Q^2$. In the coordinate representation the wavefunction (A.7) of the $M=J$ state has the following form

$$\Phi_{JJ}(q)=(f/\pi)^{1/4}\exp[-(1/2)(f+ig)q^2], \qquad (A.11)$$

where

$$f=\frac{(S^2-4P^2-4Q^2)^{1/2}}{S-2P}, \quad g=\frac{Q}{S-2P}. \qquad (A.12)$$

Thus, the linear canonical transformation (A.1) is reduced to a change of mass, force constant and phase of the wavefunction of the oscillatory motion.

References

[1] A.J. Dorney and J.K.G. Watson, J. Mol. Spectry. 42 (1972) 135.
[2] W.G. Harter and C.W. Patterson, J. Chem. Phys. 66 (1977) 4872.
[3] C.W. Patterson and W.G. Harter, J. Chem. Phys. 66 (1977) 4886.
[4] W.G. Harter and C.W. Patterson, J. Chem. Phys. 80 (1984) 4241.
[5] B.I. Zhilinskii, J. Mol. Spectry. 78 (1979) 203.
[6] G.G.D'yachenko and B.I. Zhilinskii, Opt. i Spectroskopia 51 (1981) 105, in Russian.
[7] J.T. Hougen and J.K.G. Watson, Can. J. Phys. 43 (1965) 298.
[8] I.M. Pavlichenkov, Soviet Phys. JETP 82 (1982) 5.
[9] S.G. Pang, A. Klein and R.M. Dreizler, Ann. Phys. (N.Y.) 49 (1968) 477.
[10] T. Holstein and H. Primakoff, Phys. Rev. 58 (1940) 1098.
[11] E.R. Marshalek, Phys. Rev. C11 (1975) 1426.
[12] A.R. Edmonds, Angular momentum in quantum mechanics (Princeton Univ. Press, Princeton, 1957).
[13] P.A. Braun, in: Problems of quantum theory of atoms and molecules (Nauka, Leningrad, 1981) p. 240, in Russian; Yu.F. Smirnov, S.K. Suslov and A.M. Shirokov, J. Phys. A17 (1984) 2157.
[14] S.T. Belyaev and I.M. Pavlichenkov, Nucl. Phys. A388 (1982) 505.
[15] A. Weber, ed., Raman spectroscopy of gases and liquids (Springer, Berlin, 1979).
[16] S. Yamamoto, M. Takami and K. Kuchitsu, J. Chem. Phys. 81 (1984) 3800.